Synthesis, Characterization and Electronic Structure of Trinuclear Complexes possessing a Hexathiolato-molybdenum(IV) or Hexaselenolatotungsten(IV) Core†

P. Michael Boorman,* Heinz-Bernhard Kraatz, Masood Parvez and Tom Ziegler
Department of Chemistry, University of Calgary, Calgary, Alberta T2N 1N4, Canada

Reaction of $[MoCl_4(SMe_2)_2]$ with thiolate and $[\{Cu(PPh_3)Cl\}_4]$ in toluene or chlorobenzene affords trinuclear heterobimetallic clusters $[(Ph_3P)Cu(\mu\text{-}SR)_3Mo(\mu\text{-}SR)_3Cu(PPh_3)]$ (R = C_6H_4Me-4 **2**, C_6H_4F-4 **3**, C_6H_4Cl-4 **4** or C_6H_4Br-4 **5**). In a similar synthesis using selenolate and $[WCl_4(SMe_2)_2]$ a cluster containing the novel hexaselenolatotungsten(IV) core was obtained. The identity of all compounds was confirmed by NMR spectroscopy. Recrystallization from tetrahydrofuran yields X-ray quality crystals. The crystal structure of **2** has been determined by single-crystal X-ray diffraction. The crystals are rhombohedral, space group $R\bar{3}$, with a = 14.988(5) Å, α = 107.17(3)° and Z = 1. The paramagnetic complex consists of an approximately octahedral hexathiolatomolybdenum(IV) dianion, with two parallel faces of the octahedron capped by triphenylphosphinecopper(I) cations. The Mo–Cu distance of 269.1(1) pm is indicative of some degree of metal–metal bonding. The presence of a dative bond from the d^{10} Cu to the d^2 Mo was confirmed by density functional calculations. However, the major contribution to the overall bonding energy stems from the electrostatic attraction between the two metal fragments.

The study of the co-ordination chemistry of molybdenum and tungsten with sulfur-donor ligands has been actively pursued in many laboratories, prompted largely by the relevance of such complexes to both biological[1,2] and industrial catalytic processes.[3,4] In spite of the vast amount of research that has been published on thiolate complexes of these metals, no example of a complex containing six monofunctional thiolates has been published. However, a number of arenedithiolato complexes have been reported.[5–8] Only recently the first examples of early-transition-metal mononuclear homoleptic hexaarenethiolato complexes, in this case niobium and tantalum, were reported.[9] In the broader context of sulfur ligation, the synthesis of clusters using tetrathiometalates as synthons has yielded a wide array of homo- and hetero-metallic clusters.[10] In this regard, the synthesis of cubane-like, sulfido-bridged clusters involving molybdenum and copper has attracted attention, partly as a result of suggestions that the tetrathiomolybdenum anion acts as an antagonist of the copper metabolism.[11] There has been an implicit assumption that this may be due to complexation of sulfidomolybdenum species to copper ions. In a recent communication,[12] we reported the synthesis and X-ray structure of a unique complex of tungsten, which possesses several of the features mentioned above. The trinuclear complex $[(Ph_3P)Cu(\mu\text{-}SC_6H_4Me\text{-}4)_3W(\mu\text{-}SC_6H_4Me\text{-}4)_3Cu(PPh_3)]$ **1** contains a hexathiolatotungsten(IV) core, with two parallel faces of the octahedron capped by triphenylphosphinecopper(I) cations. The W–Cu distances [2.708(1) Å] were indicative of direct metal–metal bonding. Density functional calculations were performed which confirmed that this interaction does contribute to the overall stability of the complex, although electrostatic forces are most dominant.

In this paper, we report the extension of this work in which the molybdenum analogue of **1** has been synthesised, and its structure determined. In addition, a number of other analogues have been prepared in which the ligating thiolates have been modified, and a selenolato complex of this type has also been synthesised.

† *Supplementary data available:* see Instructions for Authors, *J. Chem. Soc., Dalton Trans.*, 1993, Issue 1, pp. xxiii–xxviii.

Non-SI unit employed: eV ≈ 1.6 × 10^{-19} J.

Results and Discussion

Synthesis of $[(Ph_3P)Cu(\mu\text{-}SR)_3Mo(\mu\text{-}SR)_3Cu(PPh_3)]$ (R = C_6H_4Me-4 **2**, C_6H_4F-4 **3**, C_6H_4Cl-4 **4** *or* C_6H_4Br-4 **5**).—These complexes were prepared by a procedure similar to that reported earlier[12] for the tungsten–dicopper complex **1**. This method is similar to those used by Otsuka *et al.*[13] and by Schrock and co-workers[14] for preparing $M(SR)_4$ complexes. Addition of the appropriate thiol to a solution of $[MoCl_4(SMe_2)_2]$ in toluene (or chlorobenzene) in the presence of NEt_3 as a base yields a blue-green solution, which when treated with solid $[\{Cu(PPh_3)Cl\}_4]$ leads to the formation of the trinuclear complexes **2**–**5**. Recrystallization of **2** from tetrahydrofuran (thf) gave crystals of the solvate $[(Ph_3P)Cu(\mu\text{-}SC_6H_4Me\text{-}4)_3Mo(\mu\text{-}SC_6H_4Me\text{-}4)_3Cu(PPh_3)]\cdot 9thf$ on which an X-ray structural determination was carried out. The analogous complexes **3**–**5** were prepared so that the electronic effects of the aryl group could be probed.

Synthesis of $[(Ph_3P)Cu(\mu\text{-}SeC_6H_4Me\text{-}4)_3W(\mu\text{-}SeC_6H_4Me\text{-}4)_3Cu(PPh_3)]$ **6**.—The selenolatotungsten complex **6** was synthesized from $[WCl_4(SMe_2)_2]$, $HSeC_6H_4Me$-4 and $[\{Cu(PPh_3)Cl\}_4]$ in toluene solution with NEt_3, similar to the syntheses of **3**–**5**. To our knowledge, this complex is the first known example of a transition-metal complex co-ordinated by six homoleptic selenolates. Attempts to grow X-ray quality crystals were unfruitful, due to rapid loss of solvent of crystallization.

Attempts to extend this series of compounds, for example by replacing the copper(I) centre by Ag^I failed to produce crystalline materials, although spectroscopic evidence suggested that the synthesis was successful.

Crystal-structure Determination of Complex **2**.—The earlier determination[12] of the structure of **1** showed that it contained a homoleptic hexathiolatotungsten(IV) core with the tungsten(IV) in a distorted octahedral environment. No analogous complex of molybdenum has been reported, hence it was important to ascertain that the complexes **2**–**5** possessed the same structural features as **1**. The structure of the neutral complex **2** is shown in two different orientations in Fig. 1(*a*) and (*b*). The molecule is essentially isostructural with **1** except that, as is evident in Fig. 1(*b*), there is three-fold symmetry along the Cu–Mo–Cu vector.

The chlorobenzene solvated structure of **1** deviates from this symmetry by virtue of two of the thiolate groups in each $(\mu\text{-SR})_3$ set being compressed together. The asymmetric unit of **2** consists of only $\frac{1}{6}$th of the molecule, plus 1.5 molecules of thf. The thf molecules are disordered, one lying on a general position, with the oxygen atom occupying two positions. The other lies on an inversion centre, and is required to be disordered by virtue of the symmetry of the crystal. Both thf molecules show large thermal parameters.

The Cu–Mo distance of 269.1(1) pm is slightly longer than that observed by Otsuka and co-workers[15,16] in $[(Bu^tNC)_4Mo(\mu\text{-}SBu^t)_2CuBr]$. The Cu–Mo distance and the Cu–S–Mo bond angles (Table 1) are indicative of an attractive interaction between the metal centres, as was found for **1** [W–Cu 270.9(1) pm]. However, the S–Mo–S, P–Cu–S and S–Cu–S angles do not lend strong support to this interpretation.

Overall, therefore, the structure can be considered as an octahedral hexathiolatomolybdenum(IV) anion, capped on two parallel faces by triphenylphosphinecopper(I) cations.

In an attempt to check whether the lower symmetry of **1** was a result of solvent packing, or a more fundamental difference in the electronic structures due to replacement of tungsten by molybdenum, the thf solvate of **1** was prepared. Determination of the unit-cell parameters and the space group on the single crystal showed that it is indeed isomorphous and presumably isostructural with **2**. Hence the distortion from three-fold symmetry is due to the solvent molecules.

Assignment of ^{1}H NMR *Spectra of Complexes* **1–6**.—A common feature of the ^{1}H NMR of complexes **1–6** is the large shift range, indicative of a paramagnetic species (Fig. 2 and Table 2).[17] A characteristic of the spectra of **1–6** is the appearance of two signals with particularly large downfield shifts and in the case of the molybdenum systems a large line broadening. The lines for **1** are somewhat sharper and show coupling. Assignment of the ^{1}H NMR spectra can be made based on the crystal structures of **1** and **2**, the distances between the proton in question and the paramagnetic metal centre, intensity information and, in the case of **1**, detailed coupling information. Assignments of the ^{1}H NMR spectra of complexes **2–6** have been based on the spectral assignment for **1**. The correlation (COSY) spectrum (Fig. 2) of **1** shows that the doublet at δ 26.16 (d_1, *o*-H thiolate) is correlated with the doublet at δ 15.33 (d_2, *m*-H thiolate). The resonances due to the PPh_3 are well separated from the aromatic protons of the aryl thiolate. The triplet at δ 6.41 (t_1) is correlated with the pseudo-triplet (t_2) at δ 5.44. Based on the low intensity and the coupling to two magnetically identical protons, we assign the resonance at δ 6.41 to the *para*-protons of the PPh_3 ligands. For the *meta*-protons, coupling to two magnetically inequivalent nuclei should give rise to a doublet of doublets. However, due to overlapping signals a triplet (t_2) is observed for the *meta*-protons. This assignment is supported by the correlation of this triplet with a doublet at δ 1.59 (d_3). The intensity of this low-field doublet is half of that of the pseudo-triplet and the same as that of the triplet at δ 6.41. We assign this signal to the *ortho*-proton of the PPh_3 group. The singlet at δ 2.33 is assigned to the *p*-CH_3 of the thiolate. The spectra of complexes **2–6** are assigned accordingly. It appears that the *para* substituent on the thiolate has no significant effect on the position of the *ortho*- and *meta*-protons of the thiolate.

Compared to **1**, the selenolate analogue **6** shows a larger downfield shift for the *ortho*- and *meta*-protons of the arylselenolate. Although these two resonances are somewhat broadened and allow no measurement of coupling constants the resonances of the protons of the phosphine ligands are sharp and show the expected coupling.

The ^{1}H NMR spectra of complexes **1–6** shows that they are paramagnetic, even though there is evidence of metal–metal interaction in the crystal structures of **1** and **2**. Faraday measurements of the magnetic moments of **1** (μ_{eff} = 1.89)[12] and **2** (μ_{eff} = 2.16) compare well with known magnetic moments of W^{IV}[18] and Mo^{IV},[19] respectively. We therefore undertook a series of studies on the electronic structure of both WCu_2 and $MoCu_2$ to interpret the observed properties.

Table 1 Selected bond distances (pm) and angles (°) for compound **2**

Cu–Mo	269.1(1)	C(1)–P	182.8(5)
S–Mo	249.0(2)	C(7)–S	178.7(6)
P–Cu	220.9(4)	C(13)–C(10)	153.3(15)
S–Cu	234.8(2)	C–C in Ph rings	139.5
S–Mo–Cu	53.7(1)	C(2)–C(1)–P	117.3(1)
S–Cu–Mo	58.8(1)	C(6)–C(1)–P	122.7(1)
S–Cu–P	121.2(1)	C(1)–P–C(1′)	103.8(2)
C(1)–P–Cu	114.7(2)	C(8)–C(7)–S	122.2(2)
Cu–S–Mo	67.5(1)	C(12)–C(7)–S	117.8(2)
C(7)–S–Mo	110.5(3)	C(13)–C(10)–C(9)	119.6(8)
C(7)–S–Cu	108.5(2)	C(13)–C(10)–C(11)	120.4(8)
S–Mo–S	88.6(1)	C–C–C in Ph rings	120.0
S–Cu–S	95.5(1)		

Table 2 NMR spectroscopic data[a]

Complex	^{1}H[b,c]	^{31}P-{^{1}H}[b,d]
1	26.16 [2 H, d, *J*(HH) 6.2, *o*-H thiolate], 15.33 [2 H, d, *J*(HH) 6.2, *m*-H thiolate], 6.41 [1 H, t, *J*(HH) 7.3, *p*-H PPh_3], 5.44 [2 H, pt, *J*(HH), *m*-H PPh_3], 2.33 (3 H, s, *p*-CH_3 thiolate), 1.59 [2 H, d, *J*(HH) 6.9, *o*-H PPh_3]	−2.8
2	24.60 [2 H, br, 154, *o*-H thiolate], 12.20 [2 H, br, 13, *m*-H thiolate], 7.67 [1 H, t, *J*(HH) 6.7, *p*-H PPh_3], 6.78 (2 H, br, 25, *m*-H PPh_3), 6.62 [2 H, d, *J*(HH) 6.4, *o*-H PPh_3], −0.70 (3 H, s, *p*-CH_3 thiolate)	−3.6
3	24.49 (2 H, br, 153, *o*-H thiolate), 11.00 (2 H, br, 18, *m*-H thiolate), 7.78 (1 H, br, 15, *p*-H PPh_3), 6.77 (2 H, br, 59, *m*-H PPh_3), 6.56 (2 H, br, 16, *o*-H PPh_3)	−3.6
4	23.90 (2 H, br, 180, *o*-H thiolate), 11.66 (2 H, br, 13, *m*-H thiolate), 7.80 (1 H, br, 20, *p*-H PPh_3), 6.57 (2 H, br, 59, *m*-H PPh_3), 6.40 (2 H, br, 17, *o*-H PPh_3)	−3.5
5	24.39 (2 H, br, 139, *o*-H thiolate), 11.95 (2 H, br, 11, *m*-H thiolate), 7.83 [1 H, t, *J*(HH) 4, *p*-H PPh_3], 6.75 (2 H, br, 56, *m*-H PPh_3), 6.40 [2 H, d, *J*(HH) 5, *o*-H PPh_3]	−3.3
6	30.67 (2 H, br, 38, *o*-H selenolate), 15.82 (2 H, br, 16, *m*-H selenolate), 7.80 [1 H, t, *J*(HH) 7.8, *p*-H PPh_3], 6.57 [2 H, pt, *J*(HH), *m*-H PPh_3], 1.95 (3 H, s, *p*-CH_3 selenolate), 1.56 [2 H, d, *J*(HH) 5.5, *o*-H PPh_3]	−3.3

[a] Chemical shifts (δ) in ppm, coupling constants and linewidths in Hz; s = singlet, d = doublet, t = triplet, pt = pseudo-triplet, br = broad. [b] Measured in $CDCl_3$. [c] Referenced to $SiMe_4$. [d] Referenced to 85% H_3PO_4.

Density Functional Calculations.—The geometry of complexes **1** and **2** was idealized for the density functional calculation to possess D_3 point group symmetry, with the three-fold axis along the Cu–M–Cu vector, as shown in structure **I**. The bonding within the cluster was analysed in terms of the interaction between the two fragments $\{M(SH)_6\}^{2-}$ **II** and $\{Cu_2(PH_3)_2\}^{2+}$ **III** which gives rise to the energy level diagram shown in Fig. 3. The calculations indicate that the complex has a triplet ground state with the two unpaired electrons in the degenerate 3e set. These orbitals are made up mainly by d_{xy} and $d_{x^2-y^2}$ of the central metal with some sulfur lone pair contribution (21%). The clusters lowest unoccupied molecular orbital (LUMO) $3a_1$ is mainly molybdenum-based (70% Mo $3d_{z^2}$ and 30% sulfur lone-pair orbitals).

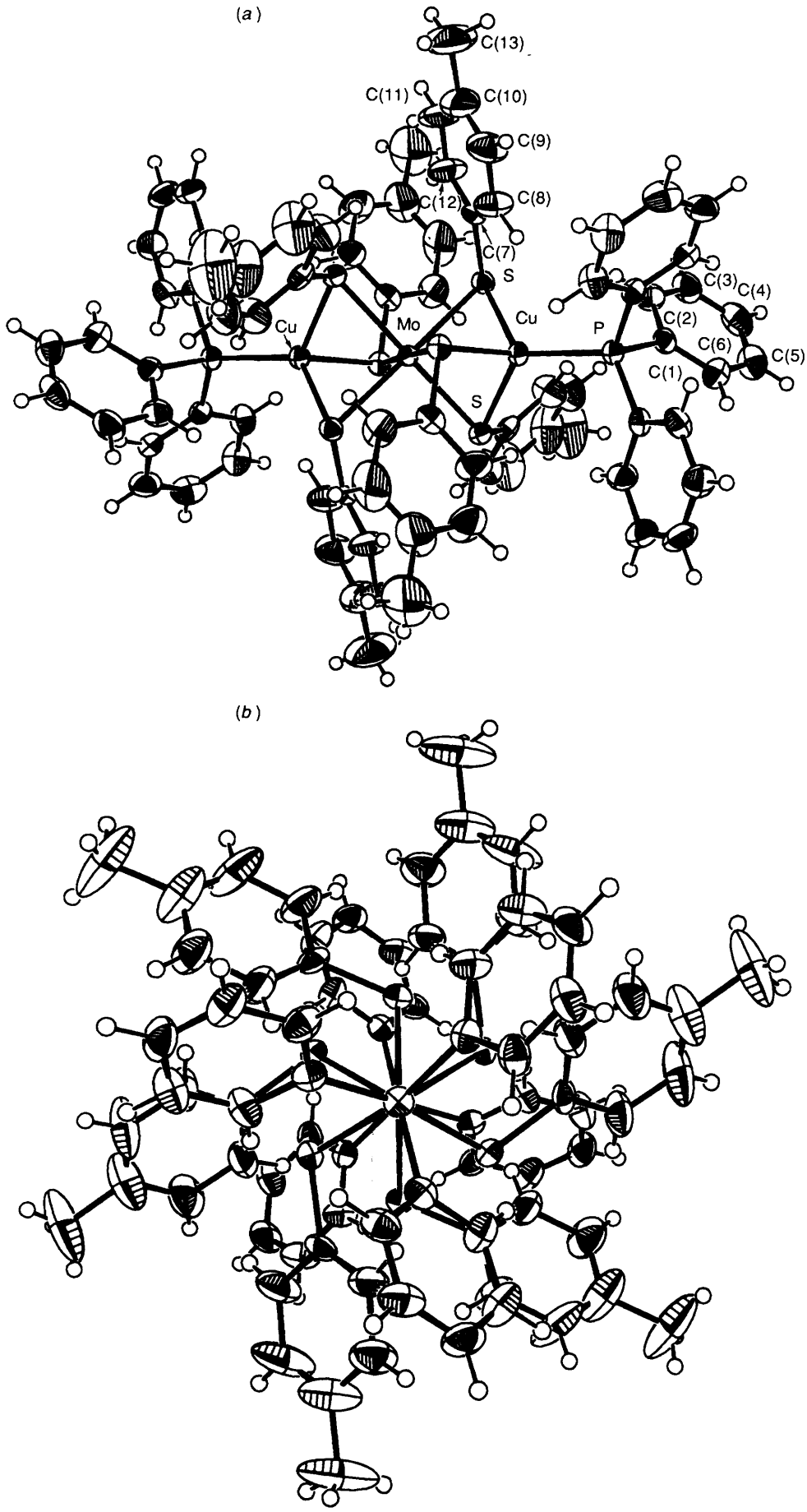

Fig. 1 (*a*) Side view of the structure of complex **2**, showing the numbering scheme. (*b*) Complex **2** as viewed down the Cu–Mo–Cu vector

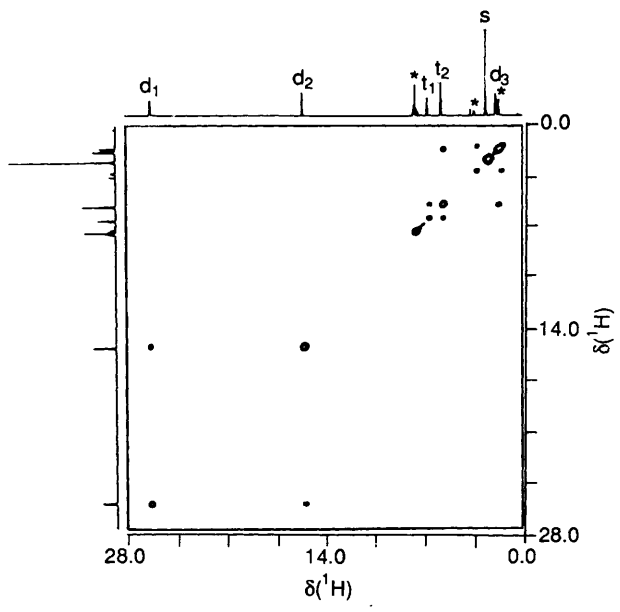

Fig. 2 COSY ^{1}H NMR spectrum ($CDCl_3$ solution) of crystalline $[(Ph_3P)Cu(\mu\text{-}SC_6H_4Me\text{-}4)_3W(\mu\text{-}SC_6H_4Me\text{-}4)_3Cu(PPh_3)]$ **1**. * Denotes impurities

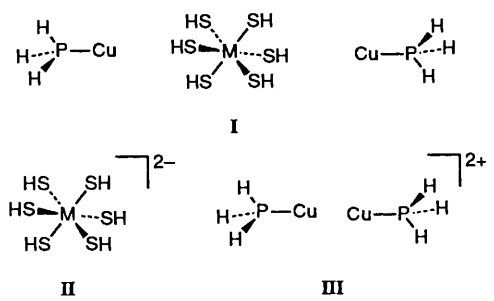

Application of the generalized transition-state method[20] allows for a detailed analysis of the interaction energy, ΔE, of the two fragments **I** and **II** in terms of steric, electronic and relativistic contributions according to equation (1) where $\Delta E^0 = [\Delta E_{elstat} + \Delta E_{exrp}]$. The steric contribution, ΔE^0, is

$$\Delta E = -(\Delta E^0 + \Delta E_{el} + \Delta E_{rel}) \quad (1)$$

composed of a purely electrostatic term, ΔE_{elstat}, and an exchange repulsion term, ΔE_{exrp}, taking into account the destabilizing two-orbital four-electron interaction between occupied orbitals on both fragments. The term ΔE_{el} represents the stabilizing contribution due to orbital interactions in the three symmetry representations between an empty orbital on one fragment and an occupied orbital on the other fragment (ΔE_{a1}, ΔE_{a2}, ΔE_e), and ΔE_{rel} is the contribution due to relativistic effects. With this, we can expand the expression for ΔE according to equation (2).

$$\Delta E = -(\Delta E_{elstat} + \Delta E_{exrp} + \Delta E_{a1} + \Delta E_{a2} + \Delta E_e + \Delta E_{rel}) \quad (2)$$

The various contributions to ΔE are given in Table 3. There is, as one might expect, a strong stabilizing electrostatic attraction between the negatively charged **II** and the positively charged **III**. In fact, electrostatic attraction is the single largest contribution to ΔE. This effect, however, is offset by repulsive interactions between d orbitals of the copper atoms of **III** and the occupied lone-pair orbitals of the sulfurs of **II**. However, the

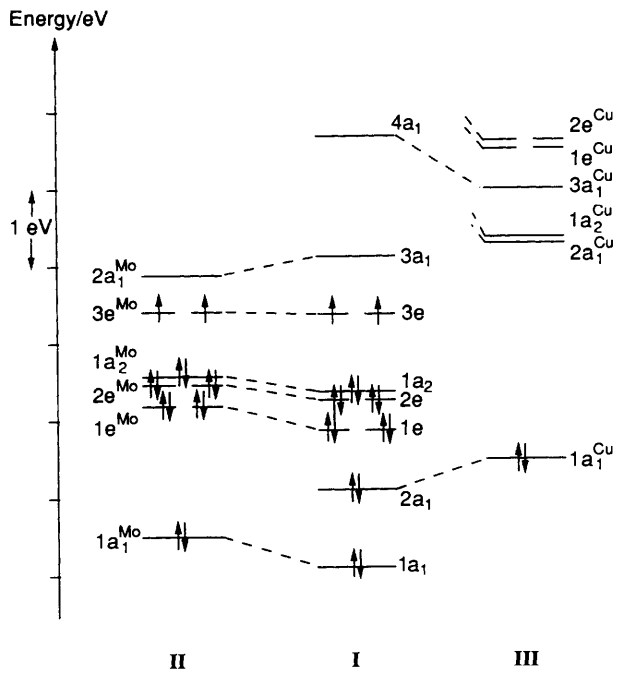

Fig. 3 Calculated molecular-orbital level diagram of the idealized model of **2**, $[(H_3P)Cu(\mu\text{-}SH)_3Mo(\mu\text{-}SH)_3Cu(PH_3)]$ **I** in D_3 point group; **II** = $\{Mo(SH)_6\}^{2-}$, **III** = $\{(H_3P)CuCu(PH_3)\}^{2+}$. The identity of the orbitals is given in structures **III**–**VIII**

overall steric contribution to ΔE is stabilizing (Mo, 496.7 kJ mol^{-1}; W, 478.5 kJ mol^{-1}).

We now turn to the orbital interactions. There are two dominant interactions in the a_1 representation. Diagram **IV** shows the interaction between the central metal fragment orbital ($1a_1^M$) being made up of occupied sulfur lone-pair orbitals and the empty 4s–4p hybrid orbital $2a_1^{Cu}$. According to Mulliken population analysis, this interaction transfers some electron density to the copper fragment (Mo, 0.2e, W, 0.30e). The second interaction, **V**, is between the occupied $1a_1^{Cu}$ orbital, made up of $3d_{z^2}$ on copper, and the empty $2a_1^M$ orbital on the central metal fragment, made up of the $4d_{z^2}$. Electron density is transferred back to the central metal fragment in this metal–metal bonding interaction (Mo, 0.32e, W, 0.31e).

Diagram **VI** shows the main interaction in the a_2 representation. Charge transfer (Mo, 0.54e, W, 0.54e) occurs from the sulfur lone pairs ($3p_z$) of the $1a_2^M$ fragment orbital to the empty sp hybrid orbital on copper of fragment **III**.

Both interactions in the e-representation, **VII** and **VIII**, involve donation of electron density from the sulfur lone-pair orbitals, $1e_x^M$ and $1e_y^M$ respectively, to the empty 4p copper orbitals, $2e_x^{Cu}$ and $2e_y^{Cu}$, of fragment **III** (Mo, 0.16e, W, 0.15e).

The metal–metal bonding interaction **V** and the bridging interactions **IV** and **VI**–**VIII** combined stabilize **I** further (Mo, 719.6 kJ mol^{-1}, W, 706.9 kJ mol^{-1}). Unfortunately, it is not possible to separate the contributions from **IV** and **V** to ΔE_{a1} and thus to assess the importance of the metal–metal bonding interaction **V** for the overall stability of the cluster. One might speculate that **IV** and **V** are of equal importance and hence **V** might contribute about 100 kJ mol^{-1} to the interaction energy ΔE. Relativistic effects are only of importance for M = W, and have been neglected for molybdenum.

UV/VIS Spectra.—The experimental data are given in the Experimental section. Most of the observed transitions are charge-transfer transitions from sulfur-based orbitals to the molybdenum-based LUMO. The complexity of the spectrum does not allow us to assign the transition from the

Table 3 Decomposition of the calculated interaction energies ΔE (in kJ mol^{-1}) between $\{M(SH_6)\}^{2-}$ and $\{Cu_2(PH_3)_2\}^{2+}$ in $[(H_3P)Cu(\mu\text{-}SH)_3M(\mu\text{-}SH)_3Cu(PH_3)]$, M = Mo or W

Complex	$-\Delta E_{elstat}$	$-\Delta E_{exrp}$	$-\Delta E_{a1}$	$-\Delta E_{a2}$	$-\Delta E_{e}$	$-\Delta E_{rel}$	ΔE^*
1	2101.3	−1622.8	218.5	165.7	322.7	38.0	1223.4
2	2105.7	−1609.0	213.4	171.5	334.7	—	1216.3

* The interaction energy ΔE is given as $\Delta E = -(\Delta E_{elstat} + \Delta E_{exrp} + \Delta E_{a1} + \Delta E_{a2} + \Delta E_{e} + \Delta E_{rel})$.

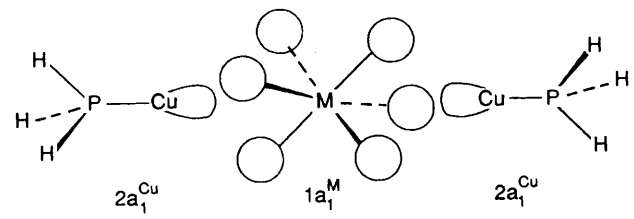

IV($1a_1$)

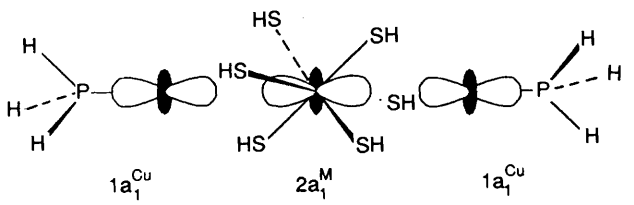

V($2a_1$)

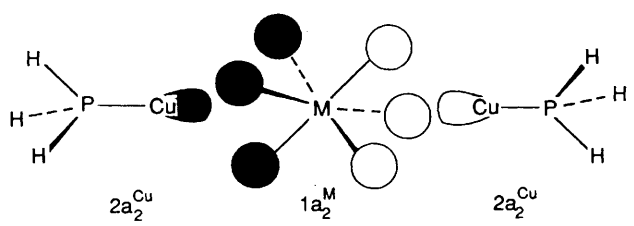

VI($1a_2$)

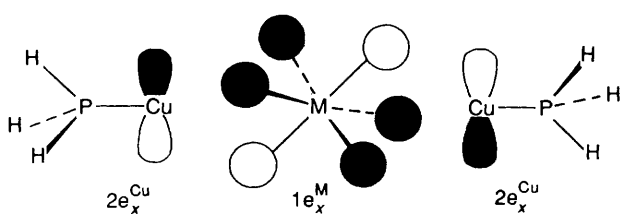

VII($1e_x$)

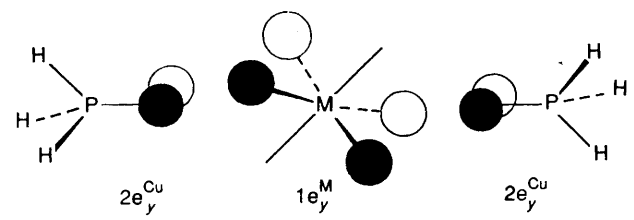

VIII($1e_y$)

molybdenum-based highest occupied molecular orbital (HOMO) to a copper-based orbital. However, the calculated value for this transition is 457 nm assuming hydrogen rather than aryl substituents are present on sulfur. The electron donating effect of the aryl group will stabilize the HOMO of the complex and hence a shift to higher wavelength is expected. Unfortunately, substitution of the aryl ring does not show the expected influence on the UV/VIS spectrum.

Conclusion

The heterobimetallic clusters **2**–**6** are synthesized in moderately high yield. The two unpaired electrons that render the complexes paramagnetic are based on the central metal (Mo for **2**–**5**). The magnetic moment of **2** compares well with known magnetic moments of molybdenum(IV) species. The density functional calculation correctly predicts the triplet ground state of the complex. The bonding within the cluster can be understood in terms of the interaction between the central $\{Mo(SR)_6\}^{2-}$ fragment and a $\{Cu_2(PPh_3)_2\}^{2+}$ fragment. Electrostatic attraction between the two fragments is the major contributor to the overall bonding energy. However, a dative bond from the d^{10} Cu to the d^2 Mo is present, similar to those known for other early–late transition-metal complexes.[21] A variation of the *para* substituent on the arylthiolate does not have any significant effect on the UV/VIS spectra of the complexes. However, preliminary electrochemical investigations suggest that an influence does exist; these results will be discussed in a future publication.

Experimental

General Procedures and Techniques.—All manipulations were carried out using standard glove-box and double manifold vacuum-line techniques under an atmosphere of dry nitrogen, or argon. Solvents were dried and degassed by standard techniques, as described previously.[22] Elemental analyses were performed by the University of Calgary Department of Chemistry Analytical Service Laboratory, and by the Canadian Microanalytical Services, Ltd. Delta, B.C., Canada. Routine ^{1}H NMR spectra were recorded on a Bruker ACE-200 spectrometer; a Bruker AM-400 (^{31}P, ^{77}Se) and a Varian XL-200 (^{31}P) spectrometer were used to record all other nuclei. UV/VIS spectra were measured in the range 200–800 nm using a Varian 219 spectrometer. IR spectra (2000–400 cm^{-1}) were recorded as KBr discs using a Mattson 4030 Galaxy Series Fourier transform IR spectrometer. The magnetic moment of **2** was measured by the Faraday method.

Synthesis of the Starting Materials.—The complexes $[WCl_4(SMe_2)_2]$[23] and $[\{Cu(PPh_3)Cl\}_4]$[24] were prepared by literature methods, $[MoCl_4(SMe_2)_2]$ was prepared from $[MoCl_4(thf)_2]$[25] by ligand replacement. The selenol $HSeC_6H_4$-Me-4 was prepared in 38% yield by a modified version of the literature procedure;[26] ^{1}H NMR ($CDCl_3$): δ 7.37, 7.33, 7.05, 7.01 (dd, AA′BB′ system, $HSeC_6H_4CH_3$), 2.30 (s, $HSeC_6H_4CH_3$) and 1.12 (s, $HSeC_6H_4CH_3$); ^{77}Se NMR ($CDCl_3$): δ 149.1 [d, J(SeH) 53 Hz].

Synthesis of $[(Ph_3P)Cu(\mu\text{-}SR)_3Mo(\mu\text{-}SR)_3Cu(PPh_3)]$ (R = C_6H_4Me-4 **2**, C_6H_4F-4 **3**, C_6H_4Cl-4 **4** *or* C_6H_4Br-4 **5**).—In a typical reaction freshly prepared $[MoCl_4(SMe_2)_2]$ (0.3 g, 0.833 mmol) was dissolved in toluene or chlorobenzene (20 cm^3) to give an orange solution which was then cooled to 0 °C.

Table 4 Final fractional coordinates (× 10^4) for non-hydrogen atoms of compound **2**

Atom	*x*	*y*	*z*
Mo	0	0	0
Cu	1619(1)	1619(1)	1619(1)
P	2949(2)	2929(2)	2949(2)
S	244(1)	1826(1)	590(1)
C(1)	3474(3)	4062(4)	2690(4)
C(2)	2775(3)	4350(4)	2132(4)
C(3)	3129(3)	5198(4)	1918(4)
C(4)	4182(3)	5760(4)	2262(4)
C(5)	4882(3)	5472(4)	2820(4)
C(6)	4528(3)	4624(4)	3035(4)
C(7)	−517(5)	2048(6)	1280(4)
C(8)	−195(5)	2228(6)	2315(4)
C(9)	−794(5)	2444(6)	2832(4)
C(10)	−1715(5)	2479(6)	2314(4)
C(11)	−2037(5)	2299(6)	1279(4)
C(12)	−1438(5)	2083(6)	762(4)
C(13)	−2394(13)	2663(17)	2874(14)

Triethylamine (0.69 cm^3, 5.0 mmol) was then slowly added from a syringe, whereupon the solution became brown. Upon addition of a solution of the appropriate thiol (5.0 mmol dissolved in 10 cm^3 of the toluene or chlorobenzene) the resulting mixture became blue-green to blue. After stirring for *ca.* 30 min at room temperature, the solution was filtered onto a solid sample of $[\{Cu(PPh_3)Cl\}_4]$ [0.5 g, equivalent to 1.67 mmol of $Cu(PPh_3)$-fragment]. A dark red-purple solution resulted, which was stirred for a further 1 h at 21 °C, and then filtered through a 2 cm pad of Celite 545. The volume of the solution was then reduced to 15 cm^3 by pumping off solvent, cooled to −20 °C, and left to stand overnight. Dark coloured crystals resulted, which upon redissolving in thf gave a purple solution. Recrystallization from thf yielded crystals of a thf solvate, suitable for an X-ray study. This was conducted for compound **2** (R = C_6H_4Me-4).

All complexes crystallize with solvent in the lattice, and the lability of this solvent rendered it difficult to obtain reproducible elemental analyses. The data presented below apply to samples that had been pumped for a prolonged time, and the calculated values assume that all the solvent (toluene, chlorobenzene or thf) had been removed. This invariably leads to some error.

(*a*) $[(Ph_3P)Cu(\mu\text{-}SC_6H_4Me\text{-}4)_3Mo(\mu\text{-}SC_6H_4Me\text{-}4)_3Cu(PPh_3)]$ **2**. Yield, 42% (Found: C, 62.90; H, 4.95; S, 12.00. Calc. for $C_{78}H_{72}Cu_2MoP_2S_6$: C, 63.00; H, 4.90; S, 12.95%). IR: 1584w, 1458vs, 1435s, 1376w, 1261w, 1180m, 1096s, 1083s, 1016s, 805vs, 744s, 694vs, 522vs, 493s and 396s cm^{-1}. UV/VIS [λ_{max}/nm (ε/dm^3 mol^{-1} cm^{-1})]: 768 (7722), 601 (3769), 526 (13 423), 469 (6137) and 416 (8086); μ_{eff} = 2.16.

(*b*) $[(Ph_3P)Cu(\mu\text{-}SC_6H_4F\text{-}4)_3Mo(\mu\text{-}SC_6H_4F\text{-}4)_3Cu(PPh_3)]$ **3**. Yield, 49% (Found: C, 57.25; H, 3.75. Calc. for $C_{72}H_{54}Cu_2F_6MoP_2S_6$: C, 57.25; H, 3.60%). IR: 1583m, 1460vs (br), 1377m, 1261w, 1180w, 1096m, 1078m, 1013w, 824s, 741m, 693m, 523m, 504m and 397w cm^{-1}. IV/VIS [λ_{max}/nm (ε/dm^3 mol^{-1} cm^{-1})]: 764 (6549), 589 (3110), 525 (11 872), 462 (5447) and 410 (7571).

(*c*) $[(Ph_3P)Cu(\mu\text{-}SC_6H_4Cl\text{-}4)_3Mo(\mu\text{-}SC_6H_4Cl\text{-}4)_3Cu(PPh_3)]$ **4**. Yield, 40% (Found: C, 52.55; H, 3.50. Calc. for $C_{72}H_{54}Cl_6Cu_2MoP_2S_6$: C, 53.75; H, 3.40%). IR: 1570w, 1470vs, 1433s, 1385m, 1262w, 1175w, 1090vs, 1008s, 814s, 745m, 694s, 540m, 523s, 492s and 373w cm^{-1}. UV/VIS [λ_{max}/nm (ε/dm^3 mol^{-1} cm^{-1})]: 747 (4029), 609 (2255), 525 (8820), 461 (4849) and 414 (6522).

(*d*) $[(Ph_3P)Cu(\mu\text{-}SC_6H_4Br\text{-}4)_3Mo(\mu\text{-}SC_6H_4Br\text{-}4)_3Cu(PPh_3)]$ **5**. Yield, 25% (Found: C, 45.25; H, 2.80. Calc. for $C_{72}H_{54}Br_6Cu_2MoP_2S_6$: C, 46.10; H, 2.90%). IR: 1561w, 1466vs, 1433s, 1379m, 1261w, 1179w, 1096vs, 1080vs, 1005vs, 808s, 745m, 694s, 523s, 498m and 361m cm^{-1}. UV/VIS [λ_{max}/nm (ε/dm^3 mol^{-1} cm^{-1})]: 767 (1823), 608 (743), 527 (3048), 465 (1409) and 418 (1880).

Synthesis of $[(Ph_3P)Cu(\mu\text{-}SeC_6H_4Me\text{-}4)_3W(\mu\text{-}SeC_6H_4Me\text{-}4)_3Cu(PPh_3)]$ **6**.—To a stirred solution of freshly prepared $[WCl_4(SMe_2)_2]$ (0.30 g, 0.66 mmol) in toluene (10 cm^3) was added NEt_3 (0.55 cm^3, 3.96 mmol). After cooling to 0 °C in an ice-bath, $HSeC_6H_4Me$-4 (0.68 g, 3.96 mmol) in toluene (10 cm^3) was added. The reaction mixture turned bright green and after stirring for 10 min it was filtered onto $[\{Cu(PPh_3)Cl\}_4]$ [0.40 g, 1.3 mmol of $Cu(PPh_3)$-fragment]. The colour of the resulting solution was green-brown, and stirring was continued for a further 10 min, after which the volume of the solution was reduced to *ca.* 10 cm^3 by pumping. The solution was then filtered and left to stand in the refrigerator at −20 °C overnight. Brown block-shaped crystals were produced (0.4 g, 33% yield) (Found: C, 50.45; H, 3.95. Calc. for $C_{78}H_{72}Cu_2P_2Se_6W$: C, 50.50; H, 3.95%). IR: 1601w, 1484vs, 1434vs, 1389w, 1261m, 1180m, 1095s, 1014s, 800vs, 743m, 693vs, 522vs, 506m and 484s cm^{-1}. UV/VIS [λ_{max}/nm (ε/dm^3 mol^{-1} cm^{-1})]: 615 (sh), 524 (4870) and 410 (5920).

X-Ray Crystal Structure of Compound **2**.—*Crystal data.* $[(Ph_3P)Cu(\mu\text{-}SC_6H_4Me\text{-}4)_3Mo(\mu\text{-}SC_6H_4Me\text{-}4)_3Cu(PPh_3)]\cdot 9C_4H_8O$ **2**, $C_{114}H_{144}Cu_2MoO_9P_2S_6$, M = 2135.76, rhombohedral, space group $R\bar{3}$, a = 14.988(5) Å, α = 107.17(3)°, U = 2790.9 $Å^3$, Z = 1, D_c = 1.271 g cm^{-3}, $F(000)$ = 1126 and μ(Mo-Kα) = 5.1 cm^{-1}.

A dark purple crystal of dimensions 0.24 × 0.30 × 0.45 mm was mounted in a glass capillary with a drop of mother-liquor. Previous attempts to collect data on crystals mounted on a glass fibre were unsuccessful, due to loss of solvent from the lattice. The crystal was subsequently mounted on an Enraf-Nonius CAD4 diffractometer, and cooled to 165 K. This temperature was maintained throughout the data collection. Accurate cell dimensions and a crystal orientation matrix were determined by a least-squares refinement of the setting angles of 25 reflections with θ in the range 10–15°. Intensity data were collected using Mo-Kα radiation by the ω–2θ scan method, with variable scan speed (0.65–6.7 °min^{-1}), scan width [(1.00 + 0.35 tanθ)°], in the range 2 < θ < 25°, and h −14 to 14, k −14 to 14 and l 0 to 17. Three reflections were monitored every 2 h of exposure time and showed no significant variations. The intensities of 2771 unique reflections were measured, of which 1951 had $I > 3\sigma(I)$, where $\sigma^2(I) = [S + 2B + 0.04(S - B)]^2$, with S = scan count and B = time-averaged background count extending 25% on each side. Data were corrected for Lorentz and polarization effects, but no absorption correction was applied.

The structure was solved by direct methods. Refinement of the structure was done by full-matrix least-squares calculations, initially with isotropic and finally with anisotropic thermal parameters for the non-hydrogen atoms of **2**, but thf solvent molecules were allowed isotropic thermal parameters. The H atoms of **2** were all located in the difference map at an intermediate stage of refinement, and these were included in subsequent cycles at idealized positions (C–H 0.95 Å), with fixed thermal parameters; H atoms of the thf molecules were ignored. Phenyl rings were constrained to be regular hexagons in the refinement. Convergence was reached at R = 0.081 and R' = 0.085. In the refinement cycles weights derived from counting statistics were used. Scattering factors were those of Cromer and Mann,[27] and allowance was made for anomalous dispersion.[28] A difference map calculated at the end of the refinement process revealed no chemically significant peaks (ρ_{max} = 0.9 e $Å^{-3}$). Computer programs used in this study were SHELX 76[29] and SHELX 86.[30] Fig. 1 was plotted using ORTEP II.[31] The final fractional coordinates for the non-hydrogen atoms in **2** are given in Table 4.

Additional material available from the Cambridge Crystallo-

graphic Data Centre comprises H-atom coordinates, thermal parameters and remaining bond lengths and angles.

Determination of the Space Group and Cell Constants for Complex **1** *when Crystallized from thf.*—The three-fold symmetry of the structure of **2** raised the question as to whether the asymmetry of the previously determined structure of **1** as the chlorobenzene solvate[12] would be affected by a change of solvent of crystallization. Hence a sample of **1** was recrystallized from thf, and gave rise to crystals with the same morphology as those of **2** from this solvent. An X-ray study of a single crystal of this new sample of **1** revealed that it is also rhombohedral, and its cell constants clearly show that it is isomorphous with **2**. This requires that the structure has the same symmetry elements, implying that the solvent is responsible for the lower symmetry observed in the structure of the chlorobenzene solvate of **1**. Crystal data: rhombohedral, space group $R\bar{3}$, $a = 14.887(10)$ Å, $\alpha = 107.01(4)°$, $U = 2746.86$ Å^3.

Density Functional Studies.—All calculations were based on approximate density functional theory within the local density approximation,[32] including Becke's[33] non-local exchange correction as well as Perdew's[34] inhomogeneous gradient correction for correlation. Use was made of the HFS-LCAO program system developed by Baerends *et al.*,[35] vectorized by Ravenek,[36] using the numerical integration scheme of Becke.[37] A double-ζ basis set[38] was used for the *n*s and *n*p shells of the main group elements. The *n*s, *n*p, *n*d, $(n + 1)$s and $(n + 1)$p shells of tungsten and molybdenum were represented by a triple-ζ Slater type orbital basis set. Electrons in lower shells were considered as core.[35]

All bonding energies were decomposed using the generalized transition state method.[20] Hence it was possible to decompose the total binding energy into contributions stemming from steric and single orbital contributions.[39]

Acknowledgements

We thank Dr. R. Yamdagni for help in obtaining spectra, and the Natural Sciences and Engineering Research Council of Canada for financial support. We also thank Professor E. J. Baerends and Professor Ravenek for a copy of their vectorized LCAO-HFS program system and the University of Calgary for access to their computing facilities.

References

1 R. L. Richards, *Chem. Ber.*, 1988, 29.
2 J. Okura, *Coord. Chem. Rev.*, 1985, **68**, 59.
3 F. E. Massoth, *Adv. Catal.*, 1978, **27**, 265.
4 R. Chianelli, *Catal. Rev. Sci. Eng.*, 1984, **26**, 361.
5 T. R. Halbert and E. I. Stiefel, *Inorg. Chem.*, 1989, **28**, 2501.
6 A. Butcher and P. C. H. Mitchell, *J. Chem. Soc., Chem. Commun.*, 1967, 176.
7 D. Sellmann and L. Zapf, *Z. Naturforsch., Teil B*, 1985, **40**, 380.
8 E. I. Stiefel, R. Eisenberg, R. C. Rosenberg and R. B. Gray, *J. Am. Chem. Soc.*, 1966, **88**, 2956.
9 S.-M. Koo, R. Bergero, A. Salifoglou, D. Coucouvanis, *Inorg. Chem.*, 1990, **29**, 4844.
10 A. Müller, D. Diemann, R. Jostes and H. Bögge, *Angew. Chem., Int. Ed. Engl.*, 1981, **20**, 934.
11 S. Sarkar and K. Mishra, *Coord. Chem. Rev.*, 1984, **59**, 239.
12 J. M. Ball, P. M. Boorman, J. F. Fait and T. Ziegler, *J. Chem. Soc., Chem. Commun.*, 1989, 722.
13 S. Otsuka, M. Kamata, K. Hirotsu and T. Higuchi, *J. Am. Chem. Soc.*, 1981, **103**, 3011.
14 M. L. Listemann, J. C. Dewan and R. R. Schrock, *J. Am. Chem. Soc.*, 1985, **107**, 7207.
15 S. Otsuka, N. Okura and N. C. Payne, *J. Chem. Soc., Chem. Commun.*, 1982, 531.
16 N. C. Payne, N. Okura and S. Otsuka, *J. Am. Chem. Soc.*, 1983, **105**, 245.
17 I. Bertini and C. Luchinat, *NMR of Paramagnetic Molecules in Biological Systems*, Benjamin/Cummings Publishing Co., Menlo Park, CA, 1986, ch. 2, pp. 19–46.
18 E. A. Allen, B. J. Brisdon and G. W. A. Fowles, *J. Chem. Soc.*, 1964, 4531.
19 E. A. Allen, K. Freenan and G. W. A. Fowles, *J. Chem. Soc.*, 1965, 1636.
20 T. Ziegler and A. Rauk, *Theor. Chim. Acta*, 1977, **46**, 1.
21 D. W. Stephan, *Coord. Chem. Rev.*, 1989, **95**, 41.
22 P. M. Boorman, X. Gao, G. K. W. Freeman and J. F. Fait, *J. Chem. Soc., Dalton Trans.*, 1991, 115.
23 P. M. Boorman, T. Chivers and K. N. Mahadev, *Can. J. Chem.*, 1975, **53**, 383; M. A. Schaefer-King and R. E. McCarley, *Inorg. Chem.*, 1973, **12**, 1972.
24 D. J. Fife, W. M. Moore and K. W. Morse, *Inorg. Chem.*, 1984, **23**, 1684.
25 J. R. Dilworth and R. L. Richards, *Inorg. Synth.*, 1990, **28**, 35.
26 H. Rheinboldt, Herstellung und Umwandlung organischer Selen- und Tellur Verbindungen, in *Methoden der Organischen Chemie*, eds. Houben, Weyl and Müller, Georg Thieme Verlag, Stuttgart, 1955, ch. 9, pp. 958–960.
27 D. T. Cromer and J. B. Mann, *Acta Crystallogr., Sect. A*, 1968, **24**, 321.
28 D. T. Cromer and D. Liberman, *J. Chem. Phys.*, 1970, **53**, 1891.
29 G. M. Sheldrick, SHELX 76, a program for crystal structure determination, University Chemical Laboratory, Cambridge, 1976.
30 G. M. Sheldrick, SHELXS 86, *Crystallographic Computing 3*, eds. G. M. Sheldrick, C. Kruger and R. Goddard, Clarendon Press, Oxford, 1985.
31 ORTEP II, C. K. Johnson, Report ORNL-5138, Oak Ridge National Laboratory, TN, 1976.
32 O. Gunnarson, I. Lundquist, *Phys. Rev. B*, 1974, **10**, 1319; 1976, **13**, 4274; O. Gunnarson, M. Johnson and I. Lundquist, *Phys. Rev.*, 1079, **20**, 3126.
33 A. Becke, *J. Chem. Phys.*, 1986, **84**, 4524; 1988, **88**, 1053.
34 J. P. Perdew, *Phys. Rev. B*, 1986, **33**, 8822; 1986, **34**, 7406 (erratum).
35 E. J. Baerends, D. E. Ellis and P. Ros, *Chem. Phys.*, 1973, **2**, 41; E. J. Baerends, Ph.D. Thesis, Frije Universiteit, Amsterdam, 1975.
36 W. Ravenek, in *Alogarithms and Applications on Vector and Parallel Computers*, eds. H. J. J. Riele, Th. J. Dekker and H. A. van de Horst, Elsevier, Amsterdam, 1987.
37 A. Becke, *J. Chem. Phys.*, 1988, **88**, 2547.
38 J. G. Snijders, E. J. Baerends and P. Vernoijs, *At. Data Nucl. Data Tables*, 1982, **26**, 483; P. Vernois, J. G. Snijders and E. J. Baerends, *Slater Type Basis Functions for the Whole Periodic Table*, Internal Report, Frije Universiteit, Amsterdam, 1981.
39 T. Ziegler, A General Energy Decomposition Scheme for the Study of Metal–Ligand Interaction in Complexes, in *Clusters and Solids*, NATO ASI, in the press.

Received 21*st August* 1992; *Paper* 2/04530C